
Absorbed Radiation Dose in Adults from Iodine-131 and Iodine-123 Orthoiodohippurate and Technetium-99m DTPA Renography

Ove Carlsen

Department of Clinical Physiology and Nuclear Medicine, Vejle Hospital, Vejle, Denmark

A mathematic model for evaluation of absorbed dose in radionuclide renography has been developed and programmed for automatic calculation in the computer. Input data to the model are readily available from the results of the renography and, hence, the method described is suitable for individual dose determinations in adults. Apart from the situation with very considerable outflow obstructions [¹³¹I]OIH single probe renography involves a 15–20 times smaller dose to radiation sensitive organs than [¹²³I]OIH gamma camera renography. Further, the latter examination results in a 2–10 times smaller dose than [^{99m}Tc]DTPA gamma camera renography under normal outflow conditions. Absorbed renal dose is large, ~70 mGy, in the three renographies in the borderline case with total outflow obstructions. For comparison, i.v. pyelography, which is the x-ray examination often used instead of radionuclide renography, involves an absorbed dose to ovaries 10–1000 times larger than in radionuclide renography.

J Nucl Med 29:400–406, 1988

A model simulating the kinetics of the radioactive indicator in the total body, kidneys, and bladder urine has been prepared for evaluation of absorbed dose in radionuclide renography. The calculations are based on the effective mean residence times of the injected dose in the above compartments and the MIRD tables of absorbed dose per unit cumulated activity for the “standard man” (*1*).

The model is designed to meet three purposes: (a) the determination of the absorbed dose in the individual renographic examination; (b) the comparison of absorbed dose in various organs for different types of radioactive indicators used in renography; and (c) the comparison of absorbed dose under various physiologic conditions (e.g., by variations of the total renal clearance, the fractional renal clearances of left and right kidney, the renal mean transit times, and the time interval between bladder voidings).

The model proposed may also be applicable in other examinations with similar kinetics of the radioactive indicator, e.g., in radionuclide hepatography with technetium-99m IDA ([^{99m}Tc]IDA) derivatives and

with total body, liver and intestines as distribution spaces for the radioactive indicator.

METHODS

Formula for Calculation of Absorbed Dose

In radionuclide renography the injected radiopharmaceutical is assumed to reside in the following three distribution spaces: (a) the blood and the extravascular volume (henceforth denoted ‘total body’); (b) the kidneys; and (c) the bladder urine.

The absorbed dose in mGy for a target, D_{tgt} , is given by the expression:

$$D_{\text{tgt}} = 4.50 \cdot (S_{\text{tgt, tb}} \cdot \text{EMRT}_{\text{tb}} + S_{\text{tgt, k}} \cdot \text{EMRT}_{\text{k}} + S_{\text{tgt, b}} \cdot \text{EMRT}_{\text{b}}) \cdot Q, \quad (1)$$

where $S_{\text{tgt, tb}}$, $S_{\text{tgt, k}}$, and $S_{\text{tgt, b}}$ denote, respectively, the absorbed dose in rad/ $\mu\text{Ci}\cdot\text{hr}$ of the radionuclide for the target in question with respect to the total body, kidneys, and bladder. The S-data are readily available from the MIRD tables of the “standard man” (*1*). EMRT_{tb} , EMRT_{k} , and EMRT_{b} denote, respectively, the effective mean residence times in min of the injected radiopharmaceutical in the total body, kidneys, and bladder. CF_{k} and CF_{b} are correction factors which take into account the mean decay of dosage Q from injection time to the arrival times at kidneys and bladder, respectively. For Q

Received Jan. 28, 1987; revision accepted Sept. 11, 1987.

For reprints contact: Ove Carlsen, MSc, PhD, Dept. of Clinical Physiology and Nuclear Medicine, Vejle Hospital, DK-7100 Vejle, Denmark.

given in MBq the factor 4.50 converts the right side of Eq. (1) into mGy.

Effective Mean Residence Time in the Total Body

First-order kinetics of the radiopharmaceutical with respect to the kidneys is assumed. Further, the distribution of the radiopharmaceutical in the total body is approximated by a two-compartment model consisting of a plasma compartment of volume V_p and an extravascular distribution volume V_e (Fig. 1). The radioactive indicator concentrations in these two compartments are denoted $C_p(t)$ and $C_e(t)$, respectively. The intercompartmental indicator clearance is F_i while the renal plasma clearance is denoted F_{pk} .

According to the two-compartment model $C_p(t)$ can be represented by a biexponential expression (2). In gamma camera renography a small region of interest is centered over the left ventricle. The recorded activity curve over this region is called the heart curve and is denoted $H(t)$. In single probe renography the heart curve is recorded by a separate probe positioned over the heart region from the ventral side. The shapes of $H(t)$ and $C_p(t)$ are assumed identical, i.e., the heart curve can be expressed as follows:

$$H(t) = H_1 \cdot \exp(\lambda_1 \cdot t) + H_2 \cdot \exp(\lambda_2 \cdot t). \quad (2)$$

Renography with an intravenous bolus injection of a radioactive indicator and recording of the heart curve can be described as a "bolus injection—output detection" type of experiment. According to the theory of stochastic tracer analysis (3) the mean residence time of the radioactive indicator in the system consisting of V_p and V_e can be calculated as the normalized mean value of the output curve (having disregarded the small normalized mean value of the bolus input curve).

Hence, the biologic mean residence time of the radioactive

indicator in the total body, $BMRT_{tb}$, is

$$BMRT_{tb} = \frac{\int_0^{\infty} t \cdot H(t) \cdot dt}{\int_0^{\infty} H(t) \cdot dt} \quad (3)$$

$$= \frac{H_1/\lambda_1^2 + H_2/\lambda_2^2}{H_1/\lambda_1 + H_2/\lambda_2},$$

and where the biexponential expression for $H(t)$ has been inserted.

Knowledge of λ_1 , λ_2 , and the ratio H_2/H_1 (denoted RH in the following) is sufficient for determination of $BMRT_{tb}$. This information is readily available from the biexponential decomposition of the heart curve in gamma camera renography as described by Carlsen et al. (2).

The effective mean residence time of the radioactive indicator in the total body, $EMRT_{tb}$, is

$$EMRT_{tb} = 1/(1/TPHYS + 1/BMRT_{tb}) \quad (4)$$

where TPHYS denotes the mean physical decay time of the radionuclide in question.

Effective Mean Residence Time in the Kidneys

The left and right fractional renal clearances are denoted FRC_l and FRC_r , respectively; the sum of FRC_l and FRC_r equals unity. The biologic mean residence times of the radioactive indicator in the left and right kidneys are denoted $BMRT_{lk}$ and $BMRT_{rk}$. The left and right kidneys are regarded as pure delay units. The MIRL formalism does not distinguish between the left and right kidney but regards them as an entirety. Hence, biologic and effective mean residence times for the left and right kidney together will be calculated (Fig. 1).

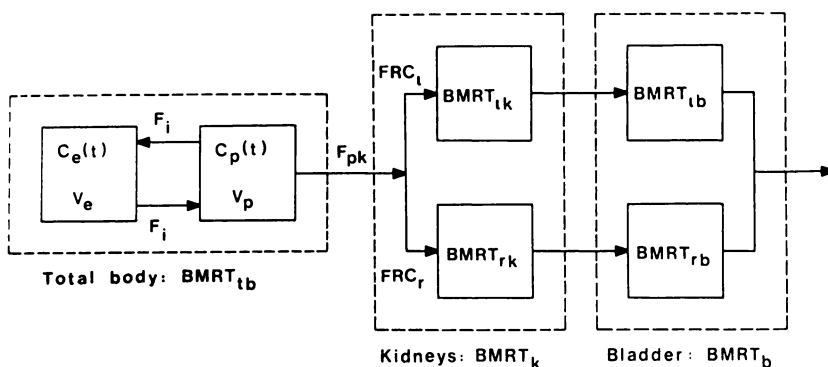


FIGURE 1

The model of prerenal indicator kinetics is an open two compartmental model consisting of a plasma compartment of volume V_p and an extravascular compartment of volume V_e . Indicator concentrations in the two compartments are $C_p(t)$ and $C_e(t)$, respectively. F_{pk} is the renal plasma clearance of indicator while F_i denotes the intercompartmental clearance of indicator. Left and right renal fractions of total renal clearance are denoted FRC_l and FRC_r , respectively. Biologic mean residence times of indicator in the left and right kidney are denoted $BMRT_{lk}$ and $BMRT_{rk}$, respectively. Biologic mean residence time for the kidneys regarded as a whole is $BMRT_k$. Bladder volume is divided into a left and right bladder volume with $BMRT_{lb}$ and $BMRT_{rb}$ denoting the biologic mean residence times of indicator, respectively. $BMRT_b$ is the biologic mean residence time of indicator for the whole bladder.

The fractional renal clearance and the biologic mean residence times of the radioactive indicator in the left and right kidney are known from deconvolution analysis of the renograms with the heart curve (2).

The effective mean residence time of radioactive indicator in the left kidney, $EMRT_{lk}$, is as follows:

$$EMRT_{lk} = (1/(1/TPHYS + 1/BMRT_{lk})). \quad (5)$$

An expression similar to Eq. (5) holds for $EMRT_{rk}$.

The effective mean residence time for the left and right kidney put together, $EMRT_k$, is:

$$EMRT_k = FRC_l \cdot EMRT_{lk} + FRC_r \cdot EMRT_{rk}. \quad (6)$$

The correction factor CF_k in Eq. (1) can be expressed as

$$CF_k = \exp(-BMRT_b/TPHYS). \quad (7)$$

Effective Mean Residence Time in the Bladder

For the present purpose it is convenient to regard the bladder urine volume as consisting of two chambers, one for the radioactive indicator originating from left kidney and the other for indicator from right kidney (Fig. 1). The corresponding biologic mean residence times are denoted $BMRT_b$ and $BMRT_{rb}$ for "left bladder" and "right bladder", respectively.

The left and right bladder curves at time t are proportional to the integral of the heart curve from zero time to time t but offset with their respective left and right renal mean transit times. Hence, the left bladder curve has a shape as in Figure 2 and is given analytically as:

$$B_l(t) = \theta \cdot FRC_l \cdot [(\exp(\lambda_1 \cdot (t - BMRT_{lk})) - 1)/\lambda_1 + RH \cdot (\exp(\lambda_2 \cdot (t - BMRT_{lk})) - 1)/\lambda_2] \quad (8)$$

with the asymptote

$$B_l(t = \infty) = \theta \cdot FRC_l \cdot (-1/\lambda_1 - RH/\lambda_2). \quad (9)$$

Expressions similar to Eqs. (8)–(9) hold for the right bladder curve, $B_r(t)$. The factor θ appearing in Eqs. (8) and (9) is a proportionality constant common to both $B_l(t)$ and $B_r(t)$. Knowledge of θ is not necessary.

The left and right bladder curves are biexponential expres-

sions like the heart curve, but only until the time when the first bladder voiding occurs at time $t = T_{lv}$ min postinjection. At this time $B_l(t)$, for example, returns to zero level and after this it continues its biexponential rise with a curve shape identical to the one as if no bladder voiding had taken place. At the subsequent bladder voidings with a time interval of ΔT_{lv} min the above pattern reiterates. The real shape of, for example, $B_l(t)$ including the effects of the bladder voidings is shown in Figure 3.

The biologic mean residence time of the radioactive indicator in the left bladder is as follows:

$$BMRT_b = \frac{\int_0^{\infty} B_l(t) \cdot dt}{B_l(t = \infty)} \quad (10)$$

With a shape of $B_l(t)$ as in Fig. 3 an analytical solution of the integral in Eq. (10) is very complicated. Numerical integration over appropriate small time steps Δt_i is far more suitable:

$$BMRT_b = \frac{\sum_{i=1}^{\infty} B_l(t_i) \cdot \Delta t_i}{B_l(t = \infty)}. \quad (11)$$

The summations in Eq. (11) are continued until the time when at least 99% of the part of the dose which eventually passes the left bladder has been voided (i.e., when $B_l(t)/B_l(t = \infty) > 0.99$ and where $B_l(t)$ is given by Eq. (8)). The proportionality constant θ in Eqs. (8)–(9) cancels out in Eq. (11).

The effective mean residence time of radioactive indicator in the left bladder, $EMRT_b$, is given by:

$$EMRT_b = (1/(1/TPHYS + 1/BMRT_b)). \quad (12)$$

An expression similar to Eq. (12) holds for $EMRT_{rb}$.

The effective mean residence time of the radioactive indicator in the bladder, $EMRT_b$, is as follows:

$$EMRT_b = FRC_l \cdot EMRT_b + FRC_r \cdot EMRT_{rb}. \quad (13)$$

The correction factors for the left and right bladder, denoted

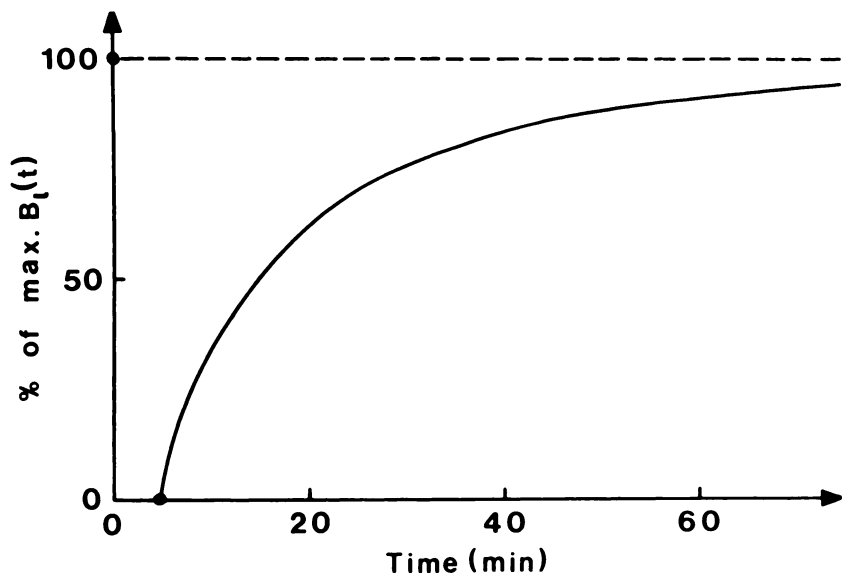


FIGURE 2

The left bladder curve, $B_l(t)$. Theoretical shape of $B_l(t)$ without bladder voidings is a biexponential expression plus a constant term and offset with a time equal to the biologic mean residence time of indicator in left kidney, $BMRT_{lk}$.

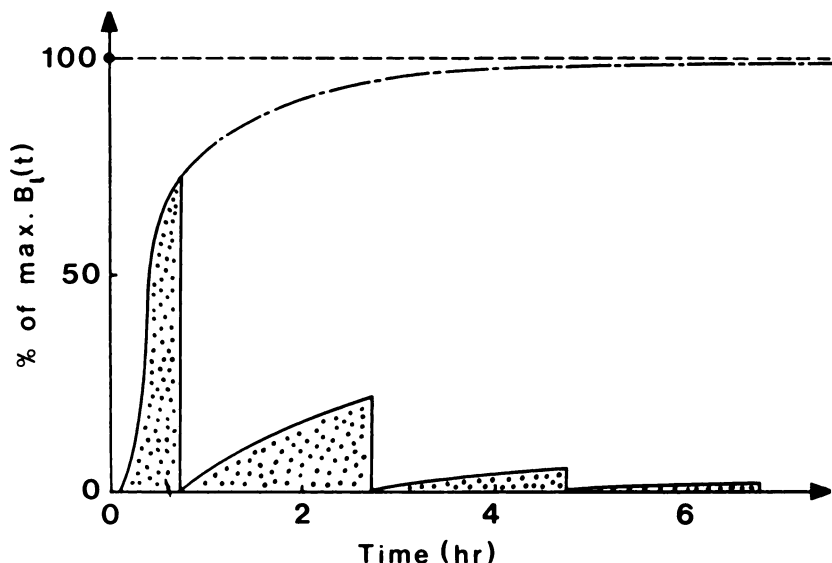


FIGURE 3
The dotted area is the area below the left bladder curve, $B_i(t)$, when bladder voidings occur at regular time intervals. Interrupted curve shows the course of $B_i(t)$ without bladder voidings.

CF_{ib} and CF_{rb} respectively, are expressed as follows:

$$CF_{ib} = \exp(-(\text{BMRT}_{ib} + \text{BMRT}_{rk})/\text{TPHYS}) \quad (14)$$

and

$$CF_{rb} = \exp(-(\text{BMRT}_{ib} + \text{BMRT}_{rk})/\text{TPHYS}) \quad (15)$$

The expression $CF_b \cdot \text{EMRT}_b$ in Eq. (1) should then be calculated as

$$CF_b \cdot \text{EMRT}_b = \text{FRC}_i \cdot CF_{ib} \cdot \text{EMRT}_{ib} + \text{FRC}_r \cdot CF_{rb} \cdot \text{EMRT}_{rb} \quad (16)$$

Mean Normal Values of Input Data

The mean normal values of input data to the absorbed dose calculations are listed in Table 1. As regards iodine-123 orthoiodohippurate (^{123}I]OIH) and iodine-131 OIH (^{131}I]OIH) the data have been derived from gamma camera renography in normal children (2). In technetium-99m diethylenetriaminepentaacetic acid (^{99m}Tc]DTPA) gamma camera renography the heart curve has hardly reached its final rate constant (i.e., λ_2) during the 40 min which is the normal duration of gamma camera renographies at our institution. Of course, the main contributions to BMRT_{ib} and BMRT_{rk} in Eqs. (3) and (10) are owing to the rate constant λ_2 . In 19 adult patients we have performed gamma camera renography with ^{99m}Tc]DTPA and GFR determination with chromium-51 ethylenetriaminetetraacetic acid (^{51}Cr]EDTA) on the same day (with GFR in the interval 20–130 ml/min/1.73 m²). The rate constant in the GFR determination, λ , was related to λ_2 as:

$$\lambda = 0.485 \cdot \lambda_2 + 0.00028 \text{ min}^{-1} \quad (17)$$

and with a correlation coefficient of 0.89. The λ -value calculated from Eq. (16) was used as the λ_2 -value in a new and modified expression for the heart curve. The new values of H_1 , H_2 , and λ_1 were determined from a set of three expressions stating that the new and old biexponential heart curve must coincide for t equal to 0, 20, and 40 min postinjection. The data for ^{99m}Tc]DTPA in Table 1 were based on biexponential decompositions of $H(t)$ in ten adults with normal GFR.

The first bladder voiding is assumed to take place within 5 min after the end of the renography and the subsequent bladder voidings at 120-min interval.

Impurities of Radioactive Indicators

Depending on the type of production of ^{123}I the radioisotope is contaminated with ^{124}I (irradiation of tellurium with protons; direct method) or ^{125}I (irradiation of iodine with protons and with xenon-123 as an intermediate product; indirect method). For the three radioactive indicators in this paper we use a radiochemical impurity of 5% and in the case of ^{123}I a radionuclide impurity of 2%. These values should be considered "worst case" situations (4,5). For ^{123}I]OIH the above impurities imply 4.9% free ^{123}I and 0.1% free ^{124}I or ^{125}I . New production methods of ^{123}I can decrease the radionuclide impurity below 0.01% (6). Radionuclide impurities of ^{131}I]OIH and ^{99m}Tc]DTPA have been ignored. For evaluation and comparison of absorbed dose without and including the impurities we have employed the effective dose equivalent. It provides a quick overview of absorbed dose using weighting factors for the various organs and tissues. Effective dose equivalents in mS valid under normal physiologic conditions are used.

TABLE 1
Mean Normal Values of Input Variables in Absorbed Dose Calculations in ^{123}I]OIH and ^{99m}Tc]DTPA Gamma Camera Renography and in ^{131}I]OIH Single Probe Renography

Item	Unit	^{123}I]OIH (^{131}I]OIH)	^{99m}Tc]DTPA
Q	MBq	37 (0.74)	185
λ_1	min ⁻¹	-0.28	-0.39
λ_2	min ⁻¹	-0.032	-0.013
RH		0.59	1.6
FRC _i		0.5	0.5
BMRT _{rk}	min	4.2	4.2
BMRT _{rk}	min	4.2	4.2
T _{uv}	min p.l.	45	45
ΔT_{uv}	min	120	120

RESULTS

The absorbed renal doses for increasing values of the biologic renal mean residence times of indicator are listed in Table 2 for the three types of renographic tests dealt with in this study. The first column corresponds to the mean normal renal BMRT values. In the remaining columns, the BMRT values have been multiplied successively by a factor of 10. The last column represents the case of bilateral total outflow obstruction.

Table 3 shows the absorbed doses in selected organs for normal and totally obstructed outflow conditions from both kidneys.

Table 4 gives a summary of absorbed doses in the bladder wall for various bladder voiding times after the end of the renographic test.

In Table 5 the effect on absorbed dose of radiochemical and radionuclide impurities of the radioactive indicators is estimated. A thyroid uptake of 35% of free iodide is assumed in the situation with impurities included. If thyroid uptake is blocked the absorbed doses in the case with impurities included are nearly the same as without impurities.

In the patient with normal renal function it is obvious from Tables 2 and 3 that the absorbed doses to radiation sensitive organs such as kidneys, ovaries, and testes are smaller in single probe renography than in gamma camera renography. The reduction in absorbed dose is at least a factor of 15 in comparison to [¹²³I]OIH and at least a factor of 35 in comparison to [^{99m}Tc]DTPA.

For increasing renal mean transit times the renal doses increase proportionately in the beginning. At extremely delayed renal passage the doses approach each other with a limit value of ~60–80 mGy. Only in the "worst case" situation does the relatively longer mean decay time of ¹³¹I involve a larger dose than renographies with ¹²³I and ^{99m}Tc. In the worst case situation the absorbed dose to the kidney is considerable for all three types of renographies. It is worth noticing that this worst case situation is nearly met under normal conditions in renal scintigraphy with [^{99m}Tc]dimercaptosuccinic acid.

As regards the absorbed dose to the bladder wall

TABLE 2
Absorbed Renal Dose (mGy) in Adults for Increasing Values of the Biologic Mean Residence Time of Radioactive Indicator in the Kidneys, BMRT_k

Type of renography	Dosage (MBq)	Absorbed dose (mGy)					
		BMRT _k					
		4.2 min	42 min	7 hr	3 d	30 d	∞
[¹²³ I]OIH	37	0.3	2	17	49	61	62
[¹³¹ I]OIH	0.74	0.02	0.2	2	17	60	83
[^{99m} Tc]DTPA	185	0.7	5	28	55	61	61

Table 4 shows at least a ten times larger dose in the two gamma camera renographies than in single probe renography. This applies to all the different bladder voiding periods mentioned in the table. The results clearly emphasize the need of encouraging the patient to void frequently during the hours after the renographic test. We use the first voiding of urine after completion of the gamma camera renography as an indirect method for detection of vesico-ureteral reflux in children (8).

DISCUSSION

The dose calculations for [^{99m}Tc]DTPA are in excellent agreement with those provided by manufacturers of DTPA kits for kidney scintigraphy under normal conditions (9). Elliott et al. (10) have studied the dosimetry of [¹²³I]OIH and [¹³¹I]OIH under normal and abnormal physiologic conditions. They conclude for both probe renography and gamma camera scintigraphy that the use of [¹²³I]OIH offers a substantial reduction in radiation dose by factors ranging from 4.5 times in the normal subjects to more than 60 times in outflow disorders. Our conclusions on absorbed dose are very different and they are based on the mean normal dose for the type of examination and not on a mGy per MBq basis as used by Elliott et al. Except for the case with total outflow obstruction, [¹³¹I]OIH single probe renography involves a considerably smaller absorbed dose than the two gamma camera renographies.

It may be argued that single probe renography has

TABLE 3
Absorbed Adult Dose (mGy) in Selected Organs for Normal and Totally Obstructed Outflow Conditions from Both Kidneys

Type of renography	Dosage (MBq)	Absorbed dose (mGy)							
		Ovaries		Testes		Bladder wall		Total body	
		N	O	N	O	N	O	N	O
[¹²³ I]OIH	37	0.080	0.3	0.050	0.03	2.0	0.08	0.030	0.6
[¹³¹ I]OIH	0.74	0.004	0.2	0.003	0.02	0.2	0.06	0.002	0.6
[^{99m} Tc]DTPA	185	0.500	0.6	0.300	0.20	5.0	0.30	0.300	0.9

N: Normal outflow. O: Total bilateral outflow obstruction.

TABLE 4

Absorbed Adult Dose (mGy) in the Bladder Wall for Various Values of the Time of First Urine Voiding, T_{uv} , and the Time Interval Between Urine Voidings, ΔT_{uv} , in Renography

T_{uv} min p.i.:	45	120	180	240	300	360
ΔT_{uv} min:	120	120	180	240	300	360
Absorbed dose (mGy)						
$[^{123}\text{I}]\text{OIH}$	2	4	6	8	10	12
$[^{131}\text{I}]\text{OIH}$	0.2	0.4	0.6	0.8	1.1	1.3
$[^{99\text{m}}\text{Tc}]\text{DTPA}$	5	6	9	12	14	17

been outdated by gamma camera renography. Screening for hydronephrosis in pregnant women is an example where the minimum radiation dose in single probe renography is of considerable importance. Another example is the screening for renal hypertension where single probe renography usually is viewed as an adequate type of examination. Owing to the poor imaging qualities of $[^{131}\text{I}]\text{OIH}$ gamma camera renography we have not taken into consideration this type of renography.

The effect of impurities (Table 5) increases the effective dose equivalent by a factor of 2 with $[^{123}\text{I}]\text{OIH}$ but by a factor of 17 with $[^{131}\text{I}]\text{OIH}$. For $[^{99\text{m}}\text{Tc}]\text{DTPA}$ the radiochemical impurity has no significant effect on the effective dose equivalent. Although a 5% radiochemical impurity is a "worst case" situation the results show for $[^{131}\text{I}]\text{OIH}$ in particular the need of keeping the impurities at a minimum level. Otherwise the advantage of having a low absorbed dose in $[^{131}\text{I}]\text{hippuran}$ single probe renography is illusory. Blocking of the thyroid gland will solve the problem with free iodide but it is not considered a recommended procedure by all experts (11).

In i.v. pyelography the absorbed dose to the ovaries is ~7.4 mGy (12), i.e., this very common x-ray examination of the upper urinary tract involves a dose at least ten times larger than radionuclide renography (even

TABLE 5

Effective Dose Equivalent (mSv) in Adults in Renography Under Normal Physiologic Conditions*

Type of renography	Dosage (MBq)	Effective dose equivalent (mSv)	
		Without impurities	Including impurities
$[^{123}\text{I}]\text{OIH}$ (direct method)	37	0.56	1.25
$[^{123}\text{I}]\text{OIH}$ (indirect method)	37	0.56	1.21
$[^{131}\text{I}]\text{OIH}$	0.74	0.036	0.62
$[^{99\text{m}}\text{Tc}]\text{DTPA}$	185	1.2	1.2

* The situations without impurities and with 5% radiochemical and 2% radionuclide (for ^{123}I) impurities are considered. Thyroid uptake of 35% of free iodide is assumed in the situations with impurities included.

with total outflow obstructions). Intravenous pyelography with externally covered testes has an absorbed dose to these glands at least three times larger than in radionuclide renography.

The individual dose calculation consisting of typing 10 input data into the computer and a computation time not exceeding 5 sec makes it an easy matter to assess the total absorbed dose in patients submitted to follow-up renographies. In the future it is not unlikely that absorbed dose calculations in some form will be required after each x-ray or radionuclide examination.

It must be emphasized that the individual dose calculations are based on S-data for the "standard man". The errors inherent in this assumption may be acceptable in adults of quasi-normal body habitus but certainly not in children. The computer program for individual dose calculation should be altered to incorporate S-data for adults other than "standard man". To our knowledge, such S-data are not yet available.

A further inaccuracy in the individual dose calculation is the fact that the voiding schedule in the individual patient is not known. If, for example, a subject with normal renal function voids the bladder immediately after the renographic test and no bladder voiding takes place for ten hours, only ~21% of the absorbed bladder wall dose occurs during the renographic examination. This applies to all three types of renographies dealt with in the paper.

The input data for $[^{131}\text{I}]\text{OIH}$ and $[^{123}\text{I}]\text{OIH}$ were derived in children over 2 yr (2). The rate constants in the biexponential formula for the heart curve in Eq. (2) are composite expressions of the ratios $-F_{pk}/V_p$, $-F_i/V_p$ and $-F_i/V_e$ (Fig. 1). Hence, these rate constants and the renal clearance rate constant are adjusted to the size of the subject (2). Our experience from several hundred renographies shows that renal mean transit times do not differ significantly between pediatric and adult normal subjects in a normal hydration state. Nor do the renal mean transit times differ in renographies with $[^{99\text{m}}\text{Tc}]\text{DTPA}$ or radioiodine hippuran. Taking into consideration the approximations involved in using the MIRD formalism, we find our input data to be applicable also in adults.

REFERENCES

1. Snyder WS, Ford MR, Warner GG, Watson SB: "S", absorbed dose per unit cumulated activity for selected radionuclides and organs, MIRD Pamphlet No 11. New York: Society of Nuclear Medicine, 1975.
2. Carlsen O, Kvinesdal B, Nathan E. Quantitative evaluation of iodine-123 hippuran gamma camera renography in normal children. *J Nucl Med* 1986; 27:117-127.
3. Lassen NA, Perl W. Tracer kinetic methods in medical physiology. New York: Raven Press, 1979: 86-88.
4. EIR Radio Isotope Service. *General and technical information*. Swiss Federal Institute for Reactor Research, CH-5303 Wuerenlingen, 1984.

5. Hammermaier A, Reich E, Bögl W. Chemical, radiochemical, and radionuclide purity of eluates from different commercial fission $^{99}\text{Mo}/^{99\text{m}}\text{Tc}$ generators. *Eur J Nucl Med* 1986; 12:41-46.
6. CYGNE. ^{123}I -hippuran and ^{133}I -pRI4. Eindhoven University of Technology, NL-5600 Eindhoven, 1986.
7. Johansson L, Mattsson S, Nosslin B: Effective dose equivalent from radiopharmaceuticals. *Eur J Nucl Med* 1984; 9:485-489.
8. Carlsen O, Lukman B, Nathan E. Indirect radionuclide renocystography for determination of vesico-ureteral reflux in children. *Eur J Nucl Med* 1986; 12:205-210.
9. Amersham International. Amerscan pentetate II technetium agent for kidney/brain scintigraphy. Amersham, United Kingdom.
10. Elliott AT, Britton KE. A review of the physiological parameters in the dosimetry of ^{123}I and ^{131}I -labelled hippuran. *Int J Appl Radiat Isot* 1978; 29:571-573.
11. Ellis RE, Nordin BEC, Tothill P, Veall N. The use of thyroid blocking agents. A report of a working party of the M.R.C. isotope advisory panel. *Br J Radiol* 1977; 50:203-204.
12. Hammer-Jacobsen E. Genetically significant radiation doses in diagnostic radiology. *Acta Radiol (Stockh)* (suppl No 222): 1963.